Schweizerische Eidgenossenschaft
Confédération suisse
Confederazione Svizzera
Confederaziun svizra

Eidgenössisches Departement fürUmwelt, Verkehr, Energie und Kommunikation UVEK

Bundesamt für Energie BFE

Final report   31st of October 2010

Magnetic heat pump with ground heat source

Optimized prototype

Auftraggeber:
Bundesamt für Energie BFE / Swiss Federal Office of Energy
Forschungsprogramm Wärmepumpen, WKK, Kälte
CH-3003 Bern
www.bfe.admin.ch

Kofinanzierung:
Direction Générale de l'Enseignement Supérieur du Canton de Vaud (DGES)
CH-1014 Lausanne
Haute Ecole d'Ingénerie et de Gestion du Canton de Vaud (HEIG-VD)
CH-1401 Yverdon-les-Bains

Auftragnehmer:
Haute Ecole d'Ingénerie et de Gestion du Canton de Vaud (HEIG-VD)
Route de Cheseaux 1
CH-1401 Yverdon
www.heig-vd.ch

Autoren:
Peter W. Egolf, HEIG-VD, IGT-SIT, Peter.egolf@heig-vd.ch
Andrej Kitanovski, University of Ljubljana, Slovenia, andrej.kitanovski@fs.uni-lj.si
Cyrill Gonin, HEIG-VD, IGT-SIT, Cyrill.gonin@heig-vd.ch
Didier Vuarnoz, Kobe University, Japan, didier_vuarnoz@yahoo.fr
Marc Diebold, HEIG-VD, IGT-SIT, marc.diebold@epfl.ch
Tom Swinnen, HEIG-VD, Tom.swinnen@heig-vd.ch
Bingfeng Yu, Jiaotong University, Xian, China, bfyu@mail.xjtu.edu.cn
Min Liu, Jiaotong University, Xian, China, minliu1983@gmail.com
Pierre Repetti, HEIG-VD, Li3C, Pierre.repetti@heig-vd.ch
Adrian Orita, HEIG-VD, Li3C, Adrian.orita@heig-vd.ch
Jean-Luc Beney, HEIG-VD, Li3C, Jean-luc.beney@heig-vd.ch

BFE-Bereichsleiter: Andreas Eckmanns, andreas.eckmanns@bfe.admin.ch
BFE-Programmleiter: Thomas Kopp, tkoppp@hsr.ch
BFE-Vertrags- und Projektnummer: 152‘928/100‘873

Abstract

In a feasibility study on magnetic heat pumps it was shown that a magnetic heat pump with a ground heat source operating in connection with a floor heating system is more ideal than a direct air/water magnetic heat pump. In this main project the objective was to plan, optimize, build and to experimentally investigate a prototype for this special domestic application.

It was decided to choose at present “best” magnetocaloric materials, which are hydrogenated Lanthanum alloys: La(Fe, Si, H). They show a very high magnetocaloric effect. On the other hand they are brittle, and therefore, at present no thin plates can be produced. Because of this, a new solution had to be found, which are specially designed high-volume-fraction packed beds containing micro tubes for the heat exchange. To obtain best results, a special heat transfer fluid of small volume was planned to be applied in the core part of the machine. Such unexpected difficulties led to a time delay in the project.

In this report the ideas concerning the high-volume-fraction bed of magnetocaloric particles, the optimization work on the heat pumping machine and the final design of the prototype are described in detail.

Representatives of the County of Vaud and the University of Applied Sciences of Western Switzerland decided – on the basis of the mentioned time delay of this research project – to stop their financial support. Caused by this decision, the second part of the project, namely the realization of the prototype and its experimental investigations, could not be realized.

Zusammenfassung

In einer Machbarkeitsstudie über magnetische Wärmepumpen wurde gezeigt, dass eine magnetische Wärmepumpe mit einer Erd-Wärme-Quelle und einem Boden-Heizungs-System idealer ist als eine direkte Luft/Wasser magnetische Wärmepumpe. In diesem Hauptprojekt waren die Ziele die Planung, die Optimierung, der Bau und die experimentelle Untersuchung eines Prototyps für diese Gebäudeanwendung.

Es wurde entschieden die zurzeit “besten” magnetokalorischen Materialien, welche hydrierte Lanthan Legierungen sind: La(Fe, Si, H), einzusetzen. Diese zeigen einen sehr grossen magnetokalorischen Effekt. Andererseits sind sie brüchig und deshalb können zurzeit aus ihnen keine dünnen Bleche produziert werden. Deswegen musste eine andere Lösung gefunden werden, welche speziell entworfene hoch voluminöse Schüttbette mit Mikro-Röhrchen für den Wärmeaustausch sind. Um beste Resultate zu erhalten wird geplant im Kernteil der Maschine ein spezielles Wärme-Austausch-Fluid mit kleinem Volumen einzusetzen. Solche unerwartete Schwierigkeiten führten zu einem zeitlichen Verzug des Forschungsprojektes.

In diesem Bericht werden die Ideen des hoch voluminösen Schüttbetts mit magnetokalorischen Teilchen, die Planung und die Optimierung der Wärmepumpe und der finale Design des Prototyps im Detail beschrieben.

Repräsentanten des Kanton Waadt und der Haute Ecole d’Ingénerie et de Gestion du Canton de Vaud haben entschieden – aufgrund der erwähnten zeitlichen Verzögerung dieses Forschungsprojekts – die finanzielle Unterstützung einzustellen. Verursacht durch diese Entscheidung konnte der zweite Teil des Projekts, nämlich die Realisierung des Prototyps und dessen experimentelle Untersuchung, nicht realisiert werden.

Résumé

Lors d'une étude de faisabilité sur les pompes à chaleur magnétiques, il a été montré l'efficacité accrue d'une pompe opérant à l'aide d'une source de chaleur froide "terre" et d'une source chaude intégrée au sol, à l'encontre d'un modèle directe "air/eau". Le cahier des charges principal de ce projet de grande envergure a consisté à optimiser et construire un prototype pour cette application domestique d'un genre innovant.

Dans ce contexte, il a été décidé de l'emploi des "meilleurs" matériaux magnétocaloriques actuels que sont les alliages de Lanthanes hydrogénés: La(Fe, Si, H). Ceux-ci adoptent un très large effet magnétocalorique. Malheureusement, ils présentent également un caractère friable et leur production sous forme de plaques fines reste aujourd'hui inenvisageable. De par ce fait, une nouvelle solution spécialement conçue pour des matériaux poreux à hauts coefficients d'occupation et intégrant des micro-tubes pour les échanges thermiques, a dû être déterminée. Afin d'obtenir les meilleurs résultats, l'utilisation au cœur de la machine d'un faible volume d'un fluide de transfert thermique non traditionnel a été planifiée. Une telle difficulté, inattendue, a conduit à des délais dans le projet.

Ce rapport traite en détails des thèmes concernant les hautes densités d'occupation volumique des matériaux magnétocaloriques poreux et le travail d'optimisation sur le prototype de pompe à chaleur. Son design final y est également entièrement décrit.

Des représentants du Canton de Vaud et de l'Université des Sciences Appliquées du Nord-Ouest Vaudois ont décidés, sur la base des délais précédemment cités, d'arrêter leurs contributions financières. Consécutivement à cette décision, la seconde partie du projet, respectivement la construction du prototype et ses dépendances expérimentales n'ont pu être réalisées.

Inhaltsverzeichnis

1. INTRODUCTION

Magnetocaloric materials in magnetic heat pumps and magnetic refrigerators are metals, which may be pure metals, sintered metals or alloys, which very often also contain rare earth materials (see e.g. conference proceedings [1] and references therein and Ref. [2]). A review on built prototypes of magnetic heat pumps and refrigerators is given in Ref. [3]. The ozone depletion potential (*ODP)* and global warming potential (*GWP)* of magnetocaloric materials are zero [4]. This is not the case for most refrigerants, which at present are applied in conventional heat pumps. In a magnetic heat pump the pressure differences can be much smaller than one bar. This is a significant advantage compared to conventional heat pumps. Their silent operation and low vibration level is further advantageous and in many cases has to be taken into consideration [4]. In magnetic heat pumps generally less moving parts are required compared to in heat pumps with a compressor. For magnetic heat pumps there exists very simple assemblies and this enables a low maintenance as well as an expectation of long life duration of a machine. In the conventional hermetic compressor heat pumps, large irreversible losses occur due to moderate compressor efficiencies (e.g. poly tropic compression, isenthalpic expansion). Furthermore, in numerous cases the motor heats up the refrigerant what may be beneficial in order to prevent liquid refrigerant to enter the compressor. But this heat is an additional burden, which needs to be rejected and leads to an additional irreversibility. Irreversibility also occurs in the regenerative heating if condensed vapour occurs. In conventional hermetic compressors the irreversible loss due to this effect may be 30 %. In an analogy between the magnetic heat pump cycle and a conventional compression heat pump cycle the magnetization of the magnetocaloric material is the analogue physical process to the compression and the demagnetization to the expansion. The two processes of magnetization and demagnetization are almost reversible. Certain losses are coupled with the hysteresis effect and eddy currents, but these may also be avoided by applying appropriate materials and design. Therefore the magnetic heat pump has a 20-30 % higher exergy efficiency compared to the conventional technology.

The project with the title: Feasibility study for magnetic heat pumps: Applications in Switzerland [5] has shown that an interesting potential is detected for magnetic brine/water heat pumps for “minergy” (minimum energy) houses with a floor heating system. In this application the two mentioned difficulties for the magnetocaloric heating technique – namely a high temperature difference between sink and source and fluctuating temperatures of these – do not occur. The study shows that, in comparison with the conventional gas-compression technology, better *COP* (<u>C</u>oefficient <u>O</u>f <u>P</u>erformance) values, but also a higher price results. Because of the environmentally benign concept, it was decided to build a prototype magnetic heat pump.

The present final report of this project contains information on the design of a magnetic heat pump operating connected to a ground heat source and a heating system. The goal of the project was the design and building of an 8 kW magnetic heat pump, which applies ground water of 5°C as heat source and with a floor heating heat sink at 35°C. These temperature levels were chosen according to the early stage of development of the magnetic heat pumping technology.

First designs were made for porous magnetocaloric heat exchangers with thin plate wavy structures. It was expected that material science would permit such after a certain period of research. These expectations were not fulfilled. The work on such structures has been published, e.g. in Ref. [5] to [8]. The efficiencies of machines with this technology are excellent. In the future such developments should be continued. This unavailability led us to develop a second good technique, namely highly packed fractal particle beds with micro tubes for the heat exchange. In this article, the main results on such designs and optimizations are presented. They were obtained by specially developed numerical tools as well as by the application of commercially available software.

2. THE MAGNETIC HEAT PUMP PROTOTYPE

2.1 Problems related to the magnetocaloric material

The largest implications on the work comes from the fact that "best" magnetocaloric materials, which at present are alloys (compounds) based on gadolinium, manganese or lanthanum are not yet so far developed to obtain very thin and large plates to create wavy structures, as it was assumed in a feasibility study (see Ref. [5]). Especially lanthanum alloys, which are chosen to build the wheel of the prototype, are rather brittle and at present impossible to apply in smooth structured form. Even more the hydrogenated alloys – which show a higher magnetocaloric effect – are still far from having the desired mechanical treatability. But some good hope is in present and future developments. This is especially the case, because up-to-present material scientists have mainly concentrated their work on the thermal properties and were hardly concerned about the mechanical treatability and stability of the considered alloys.

2.2 Lanthanum compounds

The main interest focuses on alloys of type $La(Fe_xSi_{1-x})_{13}H_y$. These materials are highly performing concerning their magnetocaloric effect. Furthermore, a large advantage is that by altering the content of hydrogen the Curie temperature can be easily shifted. This is ideal to apply the layered bed technique, which drastically improves the *COP* of a magnetic heat pump. In our case we plan to apply nine different alloys in series. Each material shall be incorporated into an own module of the cylindrical wheel. Like this a large flexibility and the possibility to easily exchange materials are given. Because at present it is impossible to obtain information on all necessary physical properties for these alloys, an approximate procedure for their determination was applied. Figures 1 and 2 shows the approximate values of the adiabatic temperature change for a 2 Tesla magnetic field change and the isothermal entropy change, respectively. Both quantities depend on the temperature of the magnetocaloric material.

2.3 The magnet and the porous magnetocaloric wheel

The magnetocaloric material is contained in a coaxial cylinder with an inner diameter D_i=100 mm and outer diameter D_o=115 mm. The length of it will be discussed in the succeeding text. The magnet assembly was designed for this kind of form by the application of the ANSYS software and in Figure 3 this is shown together with magnetic simulation results. In earlier work [5] to [8], the magnetocaloric material was considered to be shaped as a thin periodic wavy structure. Notify that magnetocaloric materials, especially also the brittle Lanthanum compounds, at present cannot be produced in such forms.

To overcome this temporal difficulty a new idea was required. This led us to a design of thin non-permeable stainless steel rings, containing a large number of micro tubes for the fluid flow with axially layered magnetocaloric particles in form of a packed bed, surrounding the micro tubes (see Figure 4).

To obtain good results the package degree of the magnetocaloric particles must be as large as possible. Our idea to solve this problem is to work with *N* generations of different well-defined particle sizes, the smaller named micro fillers. The entire *N* generation and fractal theory is presented in chapter 2.4. In an approximation to reality the cubic sphere model is shown to lead to a package degree of 74.1 %. If smaller particles are positioned with the same package structure on a finer scale into the voids, then theoretically (with only two generations of spheres) already 93 % package degree is obtained, which is almost close to a full package. Important to obtain a good performing machine is also that these packages show a

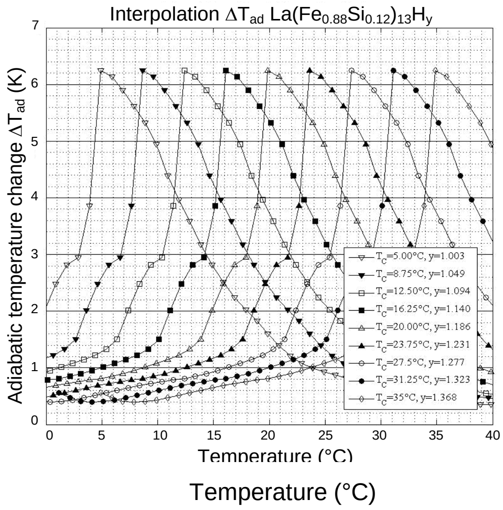

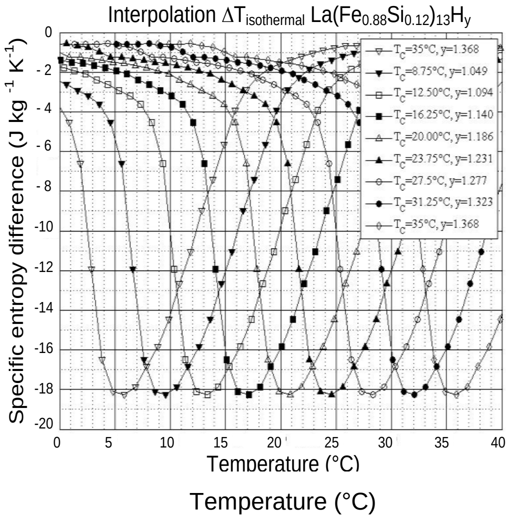

Figure 1: The series of adiabatic temperature changes – numerically determined to cover the entire span of the operation interval of the magnetic heat pump – are presented.

Figure 2: The series of specific entropy changes – determined to cover the entire span of the operation interval of the magnetic heat pump – are presented.

good thermal conductivity. If the voids are, for example, consisting of air then the thermal conductivity of the rare earth/metallic particles will substantially decrease. To obtain knowledge on the effective thermal conductivity the fractal conductivity model (FCM) – a generalization of the Maxwell-Eucken Model (MEM) for a low package degree, of the Improved Maxwell Model (IMM) for a medium package degree and of the Gonzo model (GM) for a high pa-

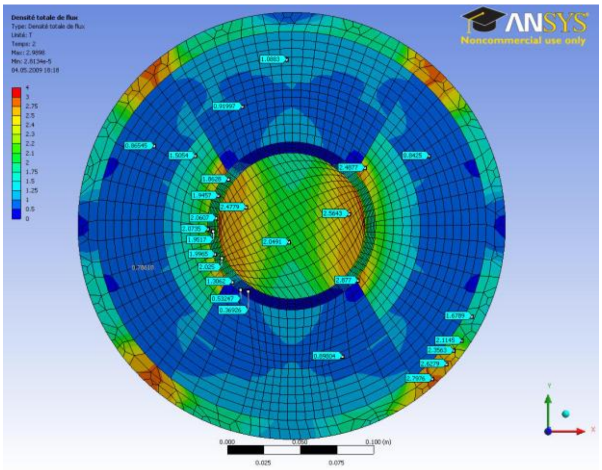

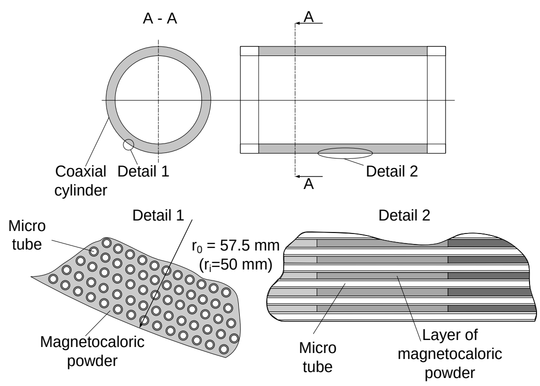

Figure 3: The front view for the magnet assembly is shown in the picture above. The highest magnetic flux density varies between 1.85 to 2.10 Tesla (see also Ref. [8]).

Figure 4: The magnetocaloric structure of the wheel of a magnetic heat pump is shown. It contains micro tubes and particles of two different sizes.

ckage degree – was derived. In order to improve the thermal conductivity of packed magnetocaloric particles, these may be suspended into liquid metal – e.g. liquid zinc, which is a good heat conductor and a magnetic non-permeable material – and then letting it solidify to obtain a bed with compact embedded particles.

2.4 The fractal package model

2.4.1 Introduction

The following treatment on fractal packed beds is also found in Ref. [9]. Packed beds (see figure 5) with a solid phase of spheres have a variety of applications in important thermal systems such as chemical reactors, thermal storage systems, heat recovery devices and combustors. Important parameters, such as the specific thermal capacity, the effective thermal conductivity and the effective thermal diffusivity in packed beds are of interest in numerous scientific investigations and engineering applications and in the design and calculation of magnetic heat pumps.

It seems impossible to develop an effective thermal conductivity model to cover all occurring conditions of different solid phases, shapes and volume fractions. Therefore, for predicting K_{eff}, different basic structure models were developed, namely the Series, Parallel, Maxwell-Eucken [10], and other effective medium models. Wang et al. [11] simulated K_{eff} of complex materials as composites with the help of such basic structure models. Numerous studies have been performed on K_{eff} of packed beds filled with a stagnant gas, including the model for regularly packed beds of rough, uniformly-sized spheres [12], the method [13] and numerical solutions [14] for mono- and poly-dispersed random assemblies of spherical particles and irregular crystals, and numerical results for polymer composites with nano and micro fillers [15]. The experimental studies of K_{eff} of packed beds with fluid flows are found in references [16-18]. Moreover, Brucker and Majdalani [19] presented K_{eff} of the most fundamental body shapes and flow configurations, under both, free and forced convection modes.

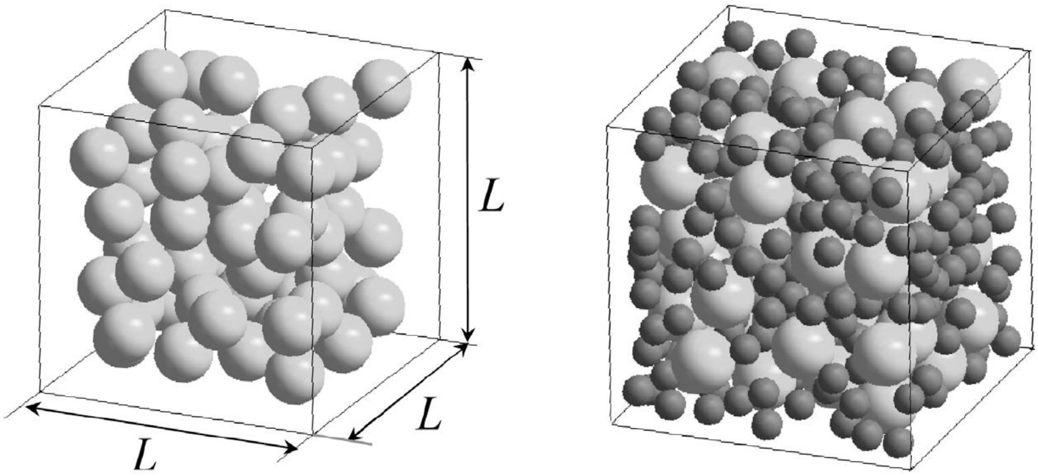

Figure 5: Random unit cells of packed spheres are shown: (a) 3-d single particle distribution, n=1; (b) a distribution with two classes of particles n=2 (from Ref. [15]).

For the case of a packed bed with spheres in a stagnant gas, the Maxwell-Eucken Model (MEM) assumes the dispersed spheres to be far apart from each other to neglect the influence of the adjacent sphere's temperature distributions. Thus the Maxwell-Eucken Model can just simulate K_{eff} of low-dense porous materials with $\psi < 10\%$. On the basis of an improved form of Maxwell's equation [20], Gonzo [21] took into account the third order of ψ and presented an Improved Maxwell Model (IMM) to predict K_{eff} of medium-dense materials ($15\% < \psi < 85\%$). Furthermore, Gonzo considered the opposed situation from the Maxwell equation and achieved the Gonzo model (GM) to study the case of high-dense materials ($\psi > 90\%$) [21]. Table 1 lists the equations of the Parallel Model (PM), MEM, IMM and GM for two-component materials. Another important contribution to effective thermal conductivities of packed beds with different volume fractions is published in reference [22]. The readers who are interested in thermal capacity of porous medium may read reference [23].

Table 1. Different models for the effective thermal conductivity of two-component materials.

Model	Effective thermal conductivity equation	Ref.	Domain
Parallel Model (PM)	$K_{\mathrm{eff,B}} = \psi_1 k_1 + (1-\psi_1) k_0$		
Max-well-Eucken Model (MEM)	$K_{\mathrm{eff,B}} = k_0 \frac{1+2\beta\psi}{1-\beta\psi},\ \beta = \frac{k_1 - k_0}{k_1 + 2k_0} = \frac{\alpha - 1}{\alpha + 2},\ \alpha = \frac{k_1}{k_0}$	[19]	Smaller than 10 %
Impro-ved Maxwell Model (IMM)	$K_{\mathrm{eff,B}} = k_0 \frac{1+2\beta\psi + (2\beta^3 - 0.1\beta)\psi^2 + 0.05\psi^3 \exp(4.5\beta)}{1-\beta\psi}$ $\beta = \frac{k_1 - k_0}{k_1 + 2k_0} = \frac{\alpha - 1}{\alpha + 2},\ \alpha = \frac{k_1}{k_0}$	[20], [21]	15 % to 85 %
Gonzo Model (GM)	$K_{\mathrm{eff,B}} = k_1 \frac{1+2\beta'(1-\psi)}{1-\beta'(1-\psi)},\ \beta' = \frac{k_0 - k_1}{k_0 + 2k_1} = \frac{1-\alpha}{1+2\alpha},\ \alpha = \frac{k_1}{k_0}$	[21]	Larger than 90 %

In some practical applications, packed beds with spheres of high volume fraction are required. Thus this final report presenting a magnetic heat pump mainly focuses on a new idea to model such packed beds and investigate important quantities, such are ψ, $c_{p,\mathrm{eff}}$ and K_{eff} of packed beds with multi-generation or even fractal features.

2.4.2 The basic idea of the multi-generation model

The physical idea is to work with different well-defined particle generations. Each generation has its own particle size. The higher the number of a particle generation is, the lower the diameter of the particles are. The generation of particles – with a certain diameter d_n – is denoted by n. The theory is derived for a large number of generations N with different particle size d_n ($1 \le n \le N$), where N even may be infinite. It is clear that from a practical point of view, only a little number of generations can be realized. The decision how many particle sizes in a practical problem are reasonable, may be taken after viewing and studying the obtained numerical results. Fig. 5 shows two examples, namely a random bed of single-sized particles and another of a bed with a two particle-size packed bed.

In the physical model, it is assumed that the largest particles (n=1) yield a well-defined package structure with voids, defined e.g. by a Bravais lattice. Furthermore, a cluster of the chosen basic package structure is then – in a strongly reduced size – packed into the remaining voids and this is repeated numerous times. This shall go on like this up to the structure with the smallest particles of size N, and if this number tends to infinity a fractal package model results.

The physical model described above can be efficiently performed if a following particle generation shows much smaller diameters. Therefore for simplicity, we only study models in the limit:

$$\frac{d_{n+1}}{d_n} \to \varepsilon > 0,\ n \in \{1,2,3,...,N-1\} \qquad (1)$$

where ε denotes a small quantity of at maximum of the order of one tenth. Practical realizations of this limit are the application of very small particles named micro fillers, respectively nano fillers [15]. In this work, we consider in the N stages of spherical particles only the special case in which all show the same basic volume fraction. This is also the one of generation n=1: ψ_1.

2.4.3 The package degree of multi-generation particle beds

With the basic features of self similarity [24], the total volume fraction of particles in the new physical model is obtained to be:

$$\begin{aligned}\psi &= \psi_1 + (1-\psi_1)\ \psi_1 + (1-\psi_1)^2 \psi_1 + ..\\ &= \psi_1 \frac{1-(1-\psi_1)^N}{1-(1-\psi_1)} = 1-(1-\psi_1)^N\end{aligned} \qquad (2)$$

2.4.4 The fractal specific heat capacity model

The basic model of the specific thermal capacity of a packed bed can be calculated by the law of weighted thermal capacities of the single components [23]:

$$c_{p,B} = \psi_1 c_{p,1} + (1-\psi_1)\, c_{p,0} \qquad (3)$$

Advantageous is that Eq. (3) has exactly the same structure as the Parallel Model in table 1. Note that, in the case where there are N generations of particles with the same basic structure in the voids, only $c_{p,0}$ shall be replaced by the term in Eq. (3) in a repetitive manner. By applying the fractal method to Eq. (3), the effective specific thermal capacity $c_{p,\mathrm{eff}}$ of a packed bed with N generations of particles is obtained:

$$\begin{aligned}c_{p,\mathrm{eff}} &= \psi_1^{(p)} c_{p,1} + \left(1-\psi_1^{(p)}\right)\cdot\\ &\cdot\left\{\psi_2^{(p)} c_{p,2} + \left(1-\psi_2^{(p)}\right)\cdot\right.\\ &\left.\cdot\left[\psi_3^{(p)} c_{p,3} + \left(1-\psi_3^{(p)}\right)(\cdots)\right]\right\}\\ &= \psi_1^{(p)} c_{p,1} + \left(1-\psi_1^{(p)}\right)\psi_2^{(p)} c_{p,2} +\\ &+ \left(1-\psi_1^{(p)}\right)\left(1-\psi_2^{(p)}\right)\psi_3^{(p)} c_{p,3} + ...\\ &\cdots + \psi_N^{(p)} c_{p,N} \prod_{n=1}^{N-1}\left(1-\psi_n^{(p)}\right) +\\ &+ c_{p,0}\prod_{n=1}^{N}\left(1-\psi_n^{(p)}\right)\end{aligned} \qquad (4)$$

If all generation particles show the same basic structure and material, the following simplification are applied:

$$c_{p,n} = c_{p,1} = \mathrm{const}\ ,\ n \in \{1,2,...,N\} \qquad (5)$$

Then Eq. (4) transforms to:

$$c_{p,\text{eff}} = \left[1-\left(1-\psi_1\right)^N\right]c_{p,1} + \left(1-\psi_1\right)^N c_{p,0} \qquad (6)$$

It should be noted that the FPM is not a suitable model to calculate the effective thermal conductivity of a packed bed with spheres. However, Eq. (6) is the accurate analytical model to derive the effective thermal capacity of such a particle bed.

2.4.5 The fractal effective thermal conductivity model

These models are the most complex ones as they are based on three different basic models as listed in table 1. The extensive mathematical equations and procedures are not outlined in this report.

The fractal continuation models related to the well known basic models for effective thermal conductivities are named with the abbreviation of the basic model, but with an additional *F* in front of it. This *F* denotes "*Fractal extended model*". So the results for the different package regimes are the Fractal Parallel Model (FPM), the Fractal Maxwell-Eucken Model (FMEM), the Fractal Improved Maxwell Model (FIMM) and the Fractal Gonzo Model (FGM). All these models are published in detail in Ref. [9].

2.4.6 The mathematical iterative procedure

In this report only the main ideas and the obtained results are presented. The details of mathematical performance, with numerous complex equations, are not given here.

The work includes models for the package degree (see chapter 2.4.3) the (effective) specific heat capacity (chapter 2.4.4) and the effective thermal conductivity (chapter 2.4.5). The first two are rather simple and therefore were presented in this report, whereas the third quantity – the effective thermal conductivity – is of higher complexity. For the porous particle beds of magnetic heat pumps these values are essential to be known.

2.4.7 Results and discussions

First test are shown for the basic models, which are listed in table 1. Figure 6a shows a comparison between model calculations and experimental data for Air-Coal and figure 6b for Air-Sand. The agreement at the two package degrees 56.3 % and 63 % are excellent.

Further numerical results are shown in figure 7. They present the effective thermal conductivities of two groups of materials, namely water-gadolinium and air-coal. The first was a calculation in the context of this project at an earlier stage, when Gadolinium was considered for an application, and the second a calculation of other materials, but with the main aim to test the model with existing experimental data. Numerical results corresponding to the different fractal models for *N* generation particles of air-coal were calculated; and these results are shown in figure 8. It is experienced that the FIMM always yields wrong results in the domain close to a full package of the bed ($\psi \to 100\%$). But this is not too astonishing as this is already the case for the results of the basic model (see $\psi \to 85\%$ in figure 6a). For all generation beds ($N \geq 1$ or $\psi_1 \leq \psi \leq 1$), our model does not only agree well with experimental results (compare with Ref. [25]) for medium-dense beds, but also shows a very good agreement in the high-number generation case. Certainly a more extended experimental verification of high generation number numerical simulation results would be very valuable.

Moreover, Figure 7 indicates, that in cases that ψ_1 is located above 55 %, only two or at maximum three generations of particles are required to achieve a high volume fraction of $\psi > 90\%$ and a maximum effective thermal conductivity.

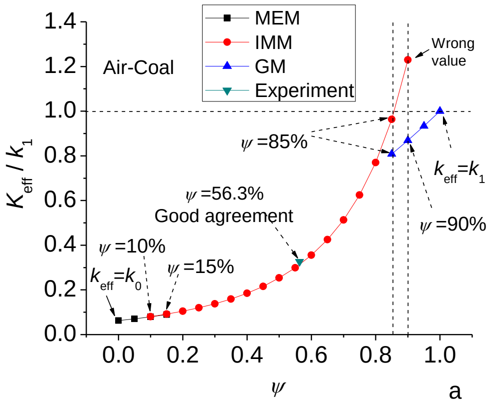

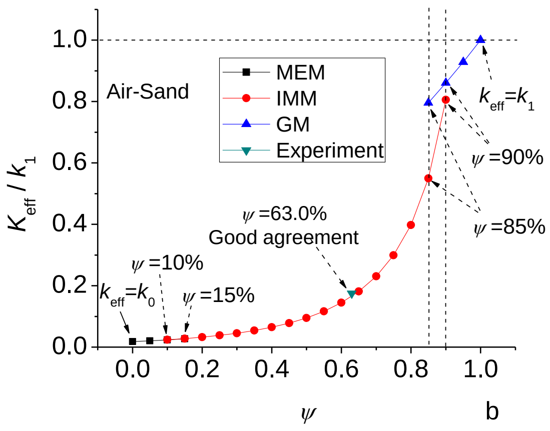

Figure 6a: Results of different basic models, here for Air-Coal, are presented.

Figure 6b: Results of different basic models, here for Air-Sand, are presented.

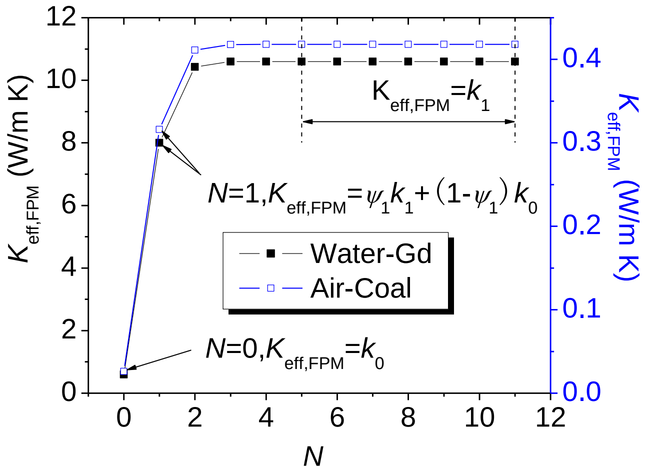

Figure 7: Numerical results of the FPM for $\psi_1 = 74\%$ for water-gadolinium and air-coal. As the package degree of this technology increases rapidly with the number of particle generations, it is expected that a fast increase is also seen in the effective thermal conductivity, and this is indeed the case. After two generations the curves already approach the constant value of the full bed. This value corresponds to the real thermal conductivity of the particles. This is a consequence that the voids are negligible small.

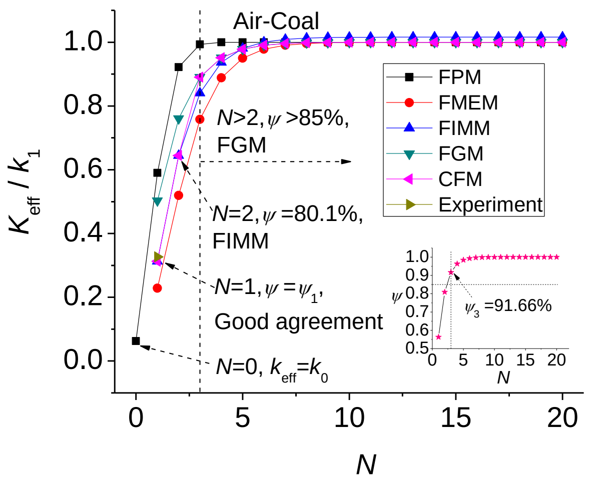

Figure 8: Numerical results for the three different fractal models of the effective thermal conductivity are presented on the right-hand side. One can clearly see that the most simple FPM shows the least good results, whereas the new developed model, which is the combination of three different basic models, shows much better agreement with experimental data.

2.4.8 Final remarks on the new models

A method to obtain high-volume fractions of packed beds is proposed. Furthermore, an analytical formula of the total volume fraction of a packed bed with *N* generation particles of the same basic structure is presented. Then a multi-generation, respectively fractal method is introduced and verified with the Parallel Model. Based on the MEM, IMM and GM, the corresponding FMEM, FIMM and FGM were derived by applying an iterative fractal-producing procedure. It should be noted that this procedure can be applied with any existing basic particle structure. Then the CFM – a combination of the FMEM, FIMM and FGM – was presented. It predicts the effective thermal conductivity K_{eff} of packed beds with *N* generation particles. Analytical solutions of $c_{p,\text{eff}}$ are also derived. Numerical results show that only two to three generations of particles are required to achieve high volume fractions ($\psi > 90\%$) of packed beds, if ψ_1 is already above 55%. If $\psi_1 > 50\%$ larger discontinuities occurring in the results in the boarder domains of the three models are avoided, and the CFM can be applied to calculate accurately K_{eff} of packed beds with *N* generation particles.

The theoretical results could only be compared with experimental data for the case *N*=1, where in a continuous phase only one particle generation is present. Well defined experiments with higher numbers of particle size generations are planned to be performed in the future.

2.5 The heat transfer fluid

Because the power of a device depends on the frequency of operation, it is evident that the magnetocaloric device has to have good heat transfer features. These depend on the geometry of the magnetocaloric structure and its thermal properties. If a packed bed with micro tubes inside is applied, it should have a very large total inner surface of the pipes and a small distance between the tubes (characteristic length of heat diffusion). In addition, an appropriate heat transfer fluid – with good thermal conductivity and specific heat – is required. The openings of the micro tubes (hydraulic diameter) must be chosen in a manner to not obtain too high pressure drops. Laminar flow is preferred to fulfil this requirement. To have a sufficient heat transfer between the material and the liquid, a good thermal conductivity of the fluid is demanded. This can be seen by studying the appropriate Nusselt relation. From the fluid dynamic and thermodynamic point-of-view, mercury would be a good heat transfer fluid. Unfortunately, it is highly toxic. If this is accepted (no-leakage system), it allows to reach very high specific powers, respectively rotation frequencies of the wheel in a machine. Liquid metal alloys with Gallium (Ga) and Indium (In) are more environmentally benign fluids (see e.g. Galinstan [28]). Galinstan is a family of eutectic alloys of gallium, indium, and tin which are liquid down to the temperature -19 °C. Due to the low toxicity and low reactivity, it is applied as a replacement for applications that previously employed toxic liquid mercury or reactive NaK (sodium-potassium alloy). Its density is 6440 kg m^{-3}, the melting point is -19°C, the dynamic viscosity 2.4 mPas (at 20°C) and the thermal conductivity 15.5 W $m^{-1}K^{-1}$ [26]. Because its thermal conductivity is very large compared to that of e.g. ethanol-water, its heat transfer in micro structures is excellent. First simulations assuming a 20 % ethanol-water solution have shown that the number of micro tubes needs to be very large in order to have an appropriate heat transfer surface, comparable with the thin periodic structures yielding micro channels (see figure 9). This figure shows in comparison the performance of a heat pump with a 20 % ethanol-water solution and the liquid metal Galinstan, respectively. For this purpose it was assumed that the package degree of the magnetocaloric particles equals 100 %. The simulation was made in a manner, that the *COP* for all the cases was *COP*~5.

Therefore, several operating parameters were varied to match the requirements. The length of the micro tubes was assumed to be 30 cm. The fluid flow in all the cases is laminar. In all cases shown in figure 9, in which the fluid Galinstan was applied, the inner diameter of a micro tube is 1 mm. This leads to equal pressure losses for the number of tubes varying between 100 and 1000. Since micro tubes fill the fixed front surface of a coaxial cylinder (see Figure 4), a higher number of tubes requires a smaller inner diameter. This diameter cannot be fixed any more at 1 mm; it must be substantially smaller (notice the limits in figure 10). In the case of e.g. 20,000 tubes, the theoretical minimum inner tube diameter is 260 mm. A much

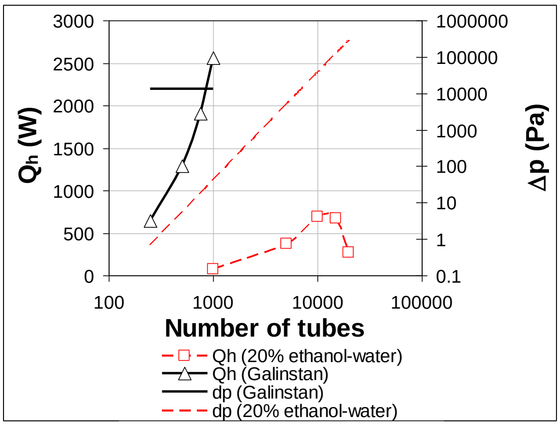

Figure 9: Heating power and the friction losses for two different liquids and a length of the micro tubes of 30 cm.

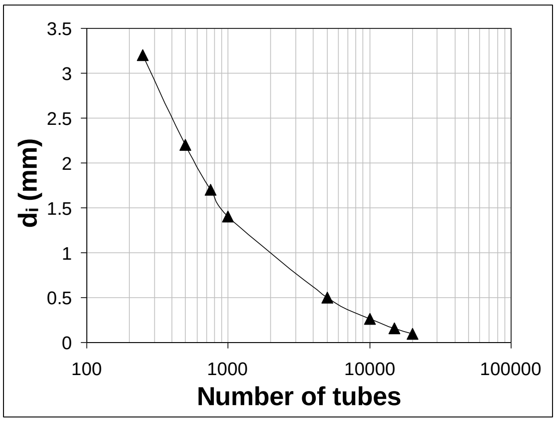

Figure 10: Ideal theoretical limits for tube diameters depending on the number of tubes (thickness *s*=0.15 mm, coaxial ring as given in Fig. 4).

larger diameter is possible for a smaller number of micro tubes. This is why in this case the pressure loss is a constant. It can be seen in figure 9 that the 20 % ethanol-water acting as heat transfer fluid cannot be efficiently applied when using micro tubes, because the heat transfer surface requires a so large number of micro tubes; and then the inner tube diameter becomes – at least from a practical point-of-view – unrealistically small. Even if the manufacturing process allows so small tubes, the pressure drop becomes enormous (this is why in figure 9 the heating power for the fixed *COP*~5 starts to rapidly decrease with the number of tubes above 10,000). In figure 9 the pressure loss of Galinstan flow is presented to be constant. This is caused by the unaltered hydraulic diameter of the tubes. The comparison shown in Figure 10 is also a hint to material scientists that they should also focus on methods that bring out magnetocaloric materials in different thin and periodic porous structures. That would permit the application of simpler and cheaper fluids, as, for example, water based solutions or brines.

3. OPTIMISATION OF THE MAGNETIC HEAT PUMP

Viewing results obtained for the liquid metal Galinstan and its influence on different heat pump characteristics, the coaxial ring was defined as shown in figure 4. In the analysis numerous parameters were varied: the volume fraction (package degree) of the magnetocaloric material (50, 75, 100 %) which surrounds the micro tubes of thicknesses (*s*=0.1, 0.2, 0.3 mm) and the number of tubes (250, 500, 750 and 1000). The analysis was performed in a manner that the *COP* was fixed. However, because the procedure required a variation of numerous parameters, the *COP* values were fixed approximately to values between *COP*=5-5.2. To adapt all data to this efficiency interval, the mass flow of the fluid and the frequency of operation were altered for all of the above listed parameters. Numerous output data was calculated: pressure loss, heating power, carry-over leakage, volume of the liquid in the structure, etc. This report presents results for the length *L*=30 cm and the number of tubes *N*= 750. The prototype will be built with four modules in a series in a manner that the system provides 8 kW heating power. The liquid metal Galinstan is expensive and by this remarkably increases the cost of a machine. Figure 11 shows the influence of the inner tube diameter on the heating power and the pressure loss. A smaller inner tube diameter (e.g. $d_i \leq 1$ mm) shows a drastic influence on the pressure drop and the heating power. Based on this it is concluded that the internal tube diameter should be kept at values of approximately 1 mm. Figure 12 shows the carry-over leakage factor depending on the package degree of the magnetocaloric material and the inner tube diameter. The carryover leakage is defined by the ratio between the time required for a fluid lump to pass through the magnetocaloric material and the time during which the magnetocaloric material rotates in the magnetic field. In our case the last one must be compared to the time required for a full rotation of the coaxial disc of 90°.

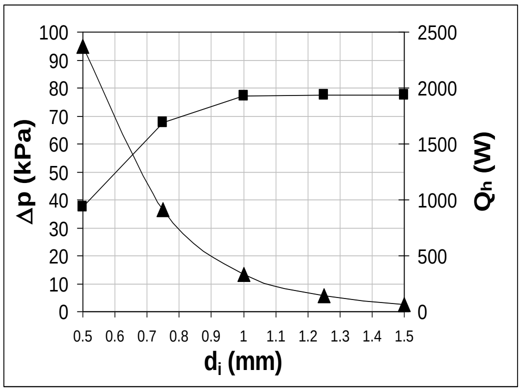

Figure 11: The pressure drop and the heating power depending on the internal diameter d_i of a tube (*COP*= 5-5.2, thickness of the tubes *s*=0.15 mm, *N*=750, *L*=30 cm).

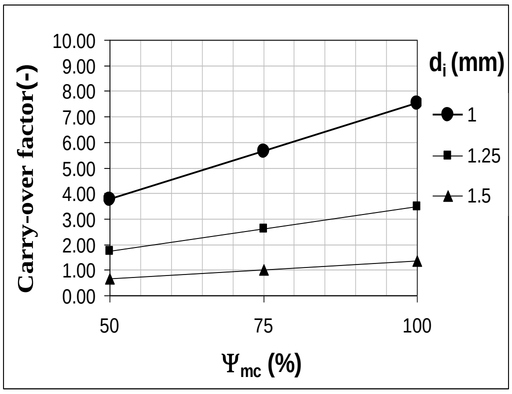

Figure 12: The carry-over factor depending on the package degree of the magnetocaloric material and the internal diameter of the tubes (*COP*=5-5.2, Q_h~2 kW, *s*= 0.15 mm, *N*=750, *L*=30 cm*)*.

As is seen in Figure 12, smaller inner tube diameters decrease the carry-over leakage. One should also take efforts to reach the highest possible package degree of particles of magnetocaloric material. This is important to have sufficient heat conduction, which was not a subject of this analysis. On the other hand, a smaller package degree of magnetocaloric material requires a higher frequency of operation (evaluated in the analysis, but not shown in this article). Figure 13 shows the overall volume fraction of the magnetocaloric material. It is the ratio between the volume of the magnetocaloric material and the total volume of the coaxial ring including the micro tubes. The package degree of the magnetocaloric material is defined to be the ratio of the volume of magnetocaloric material and of the total volume, which surrounds the micro-tubes (space that contains voids and magnetocaloric particles). A package degree of 75 % should be achieved by a proper method and application of at least two sizes

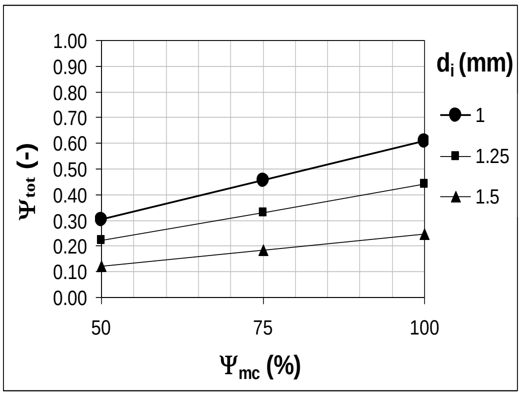

Figure 13: Total volume fraction (the volume of magnetocaloric material versus the volume of the coaxial ring) depending on the package degree of the magnetocaloric material and the internal diameter of the tubes (*COP*=5-5.2,Q_h~2 kW, *s*=0.15 mm, *N*=750, *L*=30 cm).

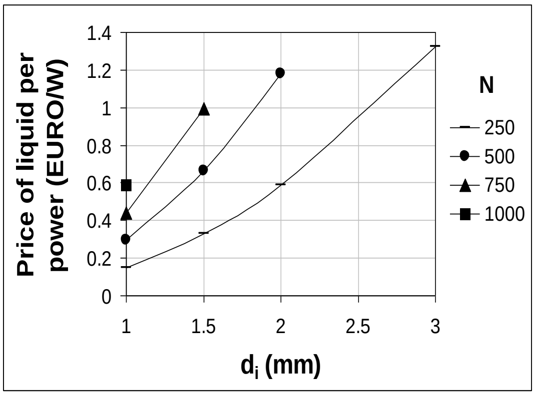

Figure 14: The specific price of the liquid metal fluid Galistan depending on the inner tube diameter and the number of tubes (*COP*=5-5.2, Q_h~2 kW, *s*=0.15 mm, *N*= 750, *L*=30 cm*)*.

of magnetocaloric particles. For the internal tube diameter d_i=1 mm and the package degree 75 %, the total volume fraction is almost 50 %. This result seems to be reasonable, especially when compared to previously obtained results for machines with wavy structures [6] to [8]. Figure 14 shows the specific price of Galinstan per heating power, depending on the inner tube diameter and the number of tubes. After some optimization, it was decided to focus on a design with N=750 tubes and an internal diameter of d_i=1 mm. This choice of parameters was also influenced by restrictions given by other parameters.

4. The design of the magnetic heat pump

In the following the state-of-the-art of our machine design is briefly reported. It actually has converged to its final stage. Smaller alterations are still possible to occur, before the building part will be initiated, but would be of small effort.

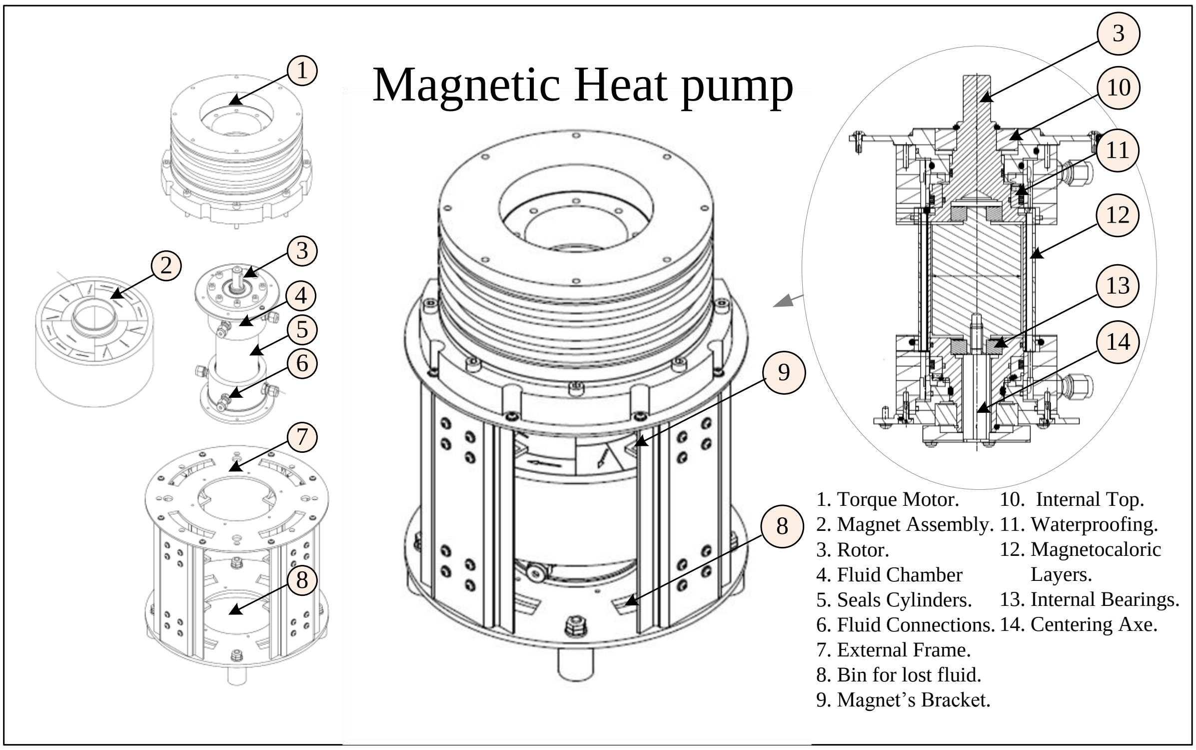

Figure 15: The compounds of the magnetic heat pump with a rotary wheel in an overview drawing. Two such modules are required for a heat pump of 4 kW and four for a heating power of 8 kW.

The prototype is of cylindrical form. It consists of the main parts: A rotor with a magnetocaloric filling, a magnet assembly, a centring axis, the fluid connections, and a motor. These, and some more details, and all their positions are shown in the overview drawing of Fig. 15.

Pointer 1 shows the position where the motor will be mounted on the top of the cylindrical machine. This motor will accelerate and decelerate the rotor part. The choice of this motor is given by its capacity to overcome the occurring moments. A heat recovery system is foreseen to recuperate the produced heat of the motor for heating purposes (not shown in the figure). The magnet's assembly (pointer 2) is composed by four zones of each 90 °. Alternatively regions of high magnetic field (approximate field strength 2 T) are alternating with such of low field (approximately 0 T). These zones are located almost homogeneously along the rotational axis of the cylinder. At the interfaces between the alternating fields large magnetic field directional derivatives occur in the azimuth direction. These changing fields are responsible for the heating – when magnetocaloric material enters the field – and cooling – when

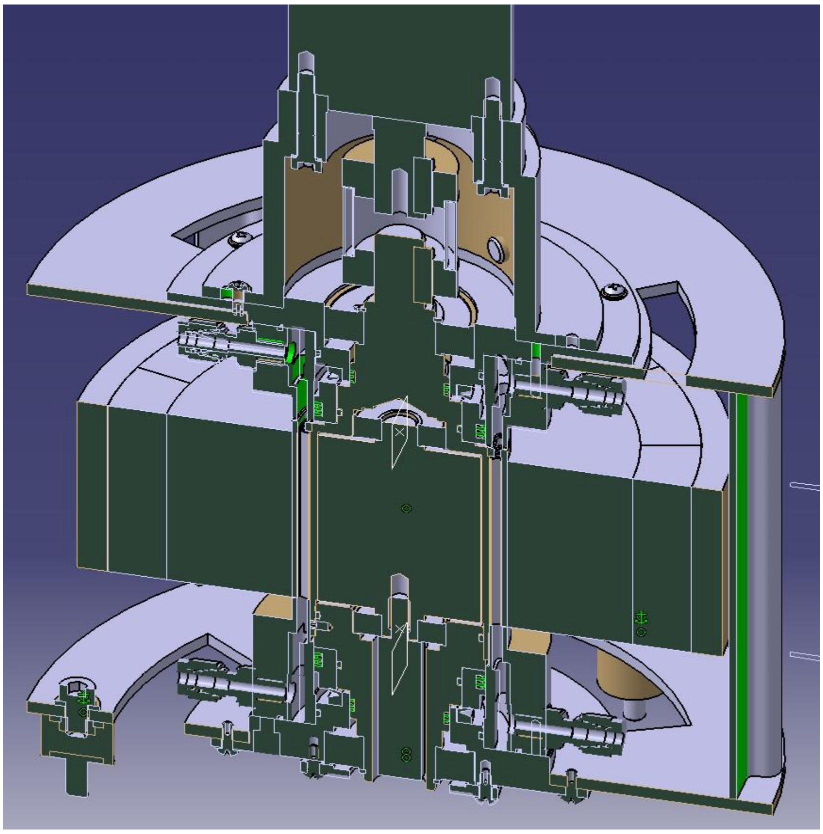

Figure 16: A three-dimensional perspective building plan is shown on the left-hand side. This machine was planned, built and optimized in a collaboration at the University of Applied Sciences of Western Switzerland between the two divisions named “Simulations des Systèmes Thermiques (SIT)” (Prof. Dr. Peter W. Egolf) and the “Laboratoire d'Ingénierie, de Conception et de CAO (Li3C)” (Prof. Pierre Repetti). The magnetocaloric wheel is built into the massive magnet’s assembly in axial direction (see the two slender channels). Furthermore, fluid connections for a convective heat transport can be seen.

magnetocaloric material exits the field. Pointer 3 shows the rotor part of the prototype. Here the heat transfer fluid passes through the magnetocaloric material beds, whereas pointer 4 denotes the fluid chambers above and below of the main cylindrical part. Between the cylinders (pointer 5), guaranteeing tightness, there are plastic protection layers, which are responsible for the corrosion protection of the magnets assembly. Furthermore, they prevent a leakage resulting by micro cracks occurring after an intense cycling in the varying magnetic field. The nine magnetocaloric materials – each filled in its own special compartment (not yet shown in Fig. 15) – posses a different Curie temperature. This temperature varies in downstream direction. They are determined by the steady-state temperature field numerically predicted to occur in the machine. The unsteady starting conditions of the magnetic heat pump is considered and solved. Furthermore, there are thin plastic cylinders between the cylinders guaranteeing the tightness (pointer 5). Pointer 6 simply shows the fluid connections, which are inlets and outlets of the liquid-metal heat transfer fluid. These standard connecting pieces allow a connection to the tubing system with a heat loss protection. Pointer 7 denotes the frame, which gives the machine its necessary stability, and pointer 8 shows a container or bin for the lost fluid. Furthermore, pointer 9 leads us to the brackets, which carry the magnet’s assembly. Different cycles are foreseen to being experimentally tested. For this the entire concept is performed in a flexible and modular manner. The covering cap inside the magnetic sleeve (pointer 10) allows an easy mounting and demounting of the prototype. The tightness of the turning pieces (pointer 11) is important and must operate with minimum friction. The tightness is guaranteed by devices containing O-rings and ceramic rings having no contact. The tightness is guaranteed with an important safety factor. The main material, namely the actual refrigerant of the magnetic heat pump, is the magnetocaloric material shown by pointer 12. Furthermore, there are numerous internal bearings (pointer 13). Last but not least a special equipment for an exact centring of the axis is foreseen and shown by pointer 14. It is responsible to adjust to ideal tolerances and to guarantee a very low friction between the turning pieces and the magnets assembly.

Further more detailed construction plans have been worked out and are any time available in the case that this machine shall be realized.

5. CONCLUSIONS AND OUTLOOK

A magnetic heat pump for a ground heat source and a floor heating system has been planned, optimized and designed. The choice was to apply a rotor consisting of magnetocaloric material instead of a rectilinear piston-type core. The second method is used by numerous researchers working with the Active Magnetic Refrigeration cycle (AMR). We decided to go another unique path and to build a machine based on the magnetic Brayton cycle and applying the layered bed technique. Very good machine efficiencies are expected for this method. This has been demonstrated by rigorous physical modelling and numerical simulations. Better coefficients of performance than for conventional heat pumps are predicted to ocur. The advantage of the rotary method is that no acceleration and deceleration work has to be performed, which is an additional loss of energy and decrease of efficiency. The magnets and the magnetocaloric wheel are essentially the most important parts concerning unknowns and economic impact on the magnetic heat pump. The design of magnets could be performed with standard knowledge on the field of electromagnetism. Not so the design of a magnetocaloric rotor (see below).

In previous work, it was assumed that material scientists would probably be able within two years to produce fine plates of magnetocaloric materials. Based on this prediction, it was decided to plan and design a magnetic heat pump on this assumption. The results for such a machine are extraordinary favourable. Unfortunately, this did not occur in time. Today material scientists concentrate on this important task and some progress has been made. But still more improvements are to be achieved. Therefore, a new direction in design, optimization and planning had to be taken. On the other hand a complete work on wavy-structure-rotor magnetic heat pumps has been performed, and almost all important results have been published (see special reference list of this project team in the remainder). Therefore, as soon as fine plates of magnetocaloric materials can be formed to wavy structures, these results can become important and maybe be applied with success.

As the sufficient heat transfer in the magnetocaloric rotor is the core problem one requires enormous high heat transfer surfaces to get a machine to be efficient. Wavy structures preformed by thin plates have (like the human lung) a tremendous inner surface per volume unit. If this is not available, another possibility to get also useful results is to take other fluids with better heat transfer properties than water has. This led to the idea of highly packed magnetoicaloric particle beds with micro tubes (such also may have a large surface, if their number is high enough) located in these beds. But such a solution is slightly less performing as the one with wavy structures and furthermore also more expensive. In a second approach a machine of this type was again planned, optimized and designed.

The research on the magnetic heat pump has been finished up to the design of the machine. Detailed plans of the unique magnetic heat pump have been carefully worked out.

As key persons of funding agencies of this project have decided to stop the financing of the project, the project team is searching for new partners for a collaboration. Good contacts to an important heat pump company at present are being established.

ACKNOWLEDGEMENTS

The authors are grateful to the Swiss Federal Office of Energy for its financial support of our research and development activities. Furthermore, we thank Thomas Kopp and Andreas Eckmanns for their scientific and administrative support of this project. A remarkable support of the education ministry of the County of Vaud in Switzerland and the University of Applied Sciences of Western Switzerland is noted.

REFERENCES CITED IN THIS REPORT

[1] K.A. Gschneidner Jr., V.K. Pecharsky, P.W. Egolf, H. Auracher, **Thermag III: The Third International Conference on Magnetic Refrigeration at Room Temperature**, May 11-15, Des Moines, IOWA, USA. International Journal of Refrigeration 33 (3) (2010), 645-647.

[2] A.M. Tishin, Y.I. Spichkin, **The magnetocaloric effect and its applications**. Institute of Physics, Series in Condensed Matter Physics, Bristol and Philadelphia, 2003.

[3] B.F.Yu, M. Liu, P.W. Egolf, A. Kitanovski, **A review of magnetic refrigerators and heat pump prototypes built before the year 2010**, Int. J. Refr. 33 (6) (2010), 1029-1060.

[4] P.W. Egolf, R.E. Rosensweig, **Magnetic refrigeration at room temperature**. 20th Informatory Note on Refrigeration Technologies of the International Institute of Refrigeration, Paris, October, 1-8, 2007.

[5] P.W. Egolf, F. Gendre, A. Kitanovski O. Sari, **Machbarkeitsstudie für magnetische Wärmepumpen: Anwendungen in der Schweiz**, Final report of the project initiated by the Swiss Federal Office of Energy, No. 100873/151017, 1- 67, 2006 (in German).

[6] A. Kitanovsk, D. Vuarnoz, M. Diebold, C. Gonin, P.W. Egolf, **Research on rotary porous wheel magnetic heat pumps in Switzerland**, 9th Int. IEA Heat Pump Conference, Zürich, Switzerland, 2008.

[7] P.W. Egolf, A. Kitanovski, D. Vuarnoz, C. Gonin, P. Repetti, A. Orita, J.-L. Beney, **Magnetische Wärmepumpe – Stand der Entwicklung**. 15. Tagung des Forschungsprogramms Umgebungswärme, Wärme-Kraft-Kopplung, Kälte des Bundesamts für Energie, 24. Juni 2009, Burgdorf, Switzerland, 59-74.

[8] P.W. Egolf, A. Kitanovski, C. Gonin, A. Nguepnang Noume, M. Liu, B.-F. Yu, P. Repetti, A. Orita, J.-L. Beney, **Magnetic heat pump with ground source – Optimized prototype**, Annual report 2009, BFE Project No. 100873.

[9] M. Liu, P.W. Egolf, B.-F. Yu, A. Kitanovski, C. Gonin, **Volume fraction, thermal capacity and effective thermal conductivity of N-number generation and fractal particle beds**, J. Mech. Eng. (accepted).

[10] J.C. Maxwell**. A Treatise on Electricity and Magnetism**, Third ed., Dover Publications Inc, New York, reprinted 1954 (Chapter 9).

[11] J.F. Wang, J.K. Carson, M.F. North, D.J. Cleland, **A new approach to modeling the effective thermal conductivity of heterogeneous material**, Int. J. Heat Mass Transfer 49 (2006), 3075-3083.

[12] M. Bahrami, M.M. Yovanovich, J.R. Culham, **Effective thermal conductivity of rough spherical packed beds**, Int. J. Heat Mass Transfer 49 (2006) 3691-3701.

[13] G.J. Cheng, A.B. Yu, P. Zulli, **Evaluation of effective thermal conductivity from the structure of a packed bed**, Chem. Eng. Sci. 54 (1999) 4199-4209.

[14] M. Kohout, A.P. Collier, F. Štěpánek, Effective thermal conductivity of wet particle assemblies, Int. J. Heat Mass Transfer 47 (2004) 5565-5574.

[15] K. Sanada, Y. Tada, Y. Shindo, **Thermal conductivity of polymer composites with close-packed structure of nano and micro fillers**, Composites: Part A 40 (2009), 724-730.

[16] M. Elsari, R. Hughes, **Axial effective thermal conductivities of packed beds**, Appl. Therm. Eng. 22 (2002), 1969-1980.

[17] E.I. Smirnov, V.A. Kuzmin, I.A. Zolotarskii, **Radial thermal conductivity in cylindrical beds packed by shaped particles**, Chem. Eng. Res. Des. 82 (2004) 293-296.

[18] R.P. Dias, C.S. Fernandes, M. Mota, J.A. Teixeira, A. Yelshin, **Permeability and effective thermal conductivity of bisized porous media,** Int. J. Heat Mass Transfer 50 (2007), 1295-1301.

[19] K.A. Brucker, J. Majdalani, **Effective thermal conductivity of common geometric shapes**, Int. J. Heat Mass Transfer 48 (2005), 4779-4796.

[20] Y.C. Chiew, E. Glandt, **The effect of structure on the conductivity of a dispersion**, J. Coll. and Int. Sci. 94 (1983) 90-104.

[21] E.E. Gonzo, **Estimating correlations for the effective thermal conductivity of granular materials**, Chem. Eng. J. 90 (2002), 299-302.

[22] P.K. Samantray, P. Karthikeyan, K.S. Reddy, **Estimating effective thermal conductivity of two-phase materials**, Int. J. Heat Mass Transfer 49 (2006), 4029-4219.

[23] A. Bouguerra, A. Ait-Mokhtar, O. Amiri, M.B. Diop, **Mesurement of thermal conductivity, thermal diffusivity and heat capacity of highly porous building material using transient plane source technique**, Int. Comm. Heat Mass Transfer 28 (2001), 1065-1078.

[24] B.B. Mandelbrot, **The Fractal Geometry of Nature**, W. H. Freeman and Company, New York, 1977.

[25] R. Krupiczka, **Analysis of thermal conductivity in granular materials**, Int. Chem. Eng. 7 (1967) 122-144.

[26] S. Masamune, J. M. Smith, **Thermal conductivity of porous catalyst pellets**, J. Chem. & Eng. Data 8 (1963) 54-58.

[27] S.W. Churchill, **The thermal conductivity of dispersions and packed beds: an illustration of the unexploited potential of limiting solution correlation**, in: A. Mujumdar, R. Mashelkar (Eds.), Advances in Transport Processes, Vol. IV, Wiley, New Delhi, 1986, pp. 394-418.

[28] **Reference Galinstan Liquids**, *Personal contact with GERATHERM MEDICAL AG,* 2009.

REFERENCES OF THE PROJECT TEAM

This final report – as other previous work – mainly contains new information and is not a summary of the entire large research project. Therefore, the following articles and reports, which have been published earlier in the context of this project, have to also be considered, if one wants to have an overview of the entire research activities. The project team (T) was also active in other similar domains as magnetic refrigeration and magnetic energy conversion. Here only the publications related to magnetic heat pumping are listed:

[T1] P. W. Egolf, F. Gendre, O. Sari, A. Kitanovski, **Magnetische Wärmepumpe für den Schweizer Markt – Machbarkeitsstudie**. 12. Tagung des Forschungsprogramms Umgebungs wärme, Wärme-Kraft-Kopplung, Kälte des Bundesamtes für Energie (BFE), 77-92, 22 Juni 2005, HTI Burgdorf.

[T2] F. Gendre, P. W. Egolf, O. Sari, **Magnetocaloric effect heat pumps in Switzerland: a feasibility study**. Proceedings of the First International Conference on Magnetic Refrigeration at Room Temperature. Montreux, Switzerland, 27-30 Sept. 2005, 347-355.

[T3] P.W. Egolf, F. Gendre, O. Sari, **Machbarkeitsstudie für magnetische Wärmepumpen: Anwendungen in der Schweiz**. Jahresbericht des Energieforschungsprogramms Umgebungswärme, Wärme-Kraft-Kopplung, Kälte, 5. Dezember 2005.

[T4] A. Kitanovski, P.W. Egolf, **The Thermodynamics of Magnetic Refrigeration.** Review article of the Int. J. Refr., 29 (2006), 3-21.

[T5] O. Sari, P.W. Egolf, N. Erbeau, F. Gendre, **Refrigeration et Pompes à Chaleur magnetiques de l'Institut de Genie Thermique à Yverdon-les-Bains**. Le Frigorist No. 28 (2006), 41.

[T6] P.W. Egolf, **Magnetic heating and refrigeration : A new technology of heat and cold production**. Invited presentation. Proceedings of the 16ème « Journée du Centre Universitaire d'Etudes des Problèmes de l'Energie (CUEPE): Le Froid pour l'alimentation et la santé : quels enjeux ?», Colloque du Cycle de formation du Cuepe 2005-2006, 6. April 2006, 45-69.

[T7] P.W. Egolf, O. Sari, F. Gendre, **Close-to-Carnot-cycle magnetic refrigerators and heat pumps: Analytical machine design and optimization**. Invited presentation at the Jubilee XX NMMM (New Magnetic Materials of Microelectronics) Conference Proceedings, Russian Association of Magnetism, Lomonosov State University, Moscow, 12-16 June 2006, AII-02, 206.

[T8] P.W. Egolf, F. Gendre, A. Kitanovski, O. Sari, **Machbarkeitsstudie für magnetische Wärmepumpen: Anwendungen in der Schweiz**. Final report for the Swiss Federal Office of Energy, No. 100873/151017, 2006, 1- 67.

[T9] P.W. Egolf, F. Gendre, A. Kitanovski, O. Sari, **Magnetic heat pumps - An approximate energy efficiency and cost study: Part I.** Proceedings of the Second IIF-IIR International Conference on Magnetic Refrigeration at Room Temperature, Portorosz, Slovenia, 11-13 April 2007, 391-398.

[T10] P.W. Egolf, F. Gendre, A. Kitanovski, O. Sari, **Magnetic heat pumps - An approximate energy efficiency and cost study: Part II**. Proceedings of the Second IIF-IIR International Conference on Magnetic Refrigeration at Room Temperature, Portorosz, Slovenia, 11-13 April 2007, 399-408.

[T11] P. W. Egolf, F. Gendre, O. Sari, A. Kitanovski, **Eine Studie über eine magnetische Wärmepumpe für ein Erdregister-Fussboden-Heizungs-System**. 14. Tagung des Forschungsprogramms Umgebungswärme, Wärme-Kraft-Kopplung, Kälte des Bundesamtes für Energie (BFE), HTI Burgdorf, 2007, 47-53.

[T12] D. Vuarnoz, A. Kitanovski, M. Diebold, P.W. Egolf, **A magnetic heat pump with porous magneto caloric material.** International Symposim on Advanced Magnetic Materials and Applications, ISAMMA, 28 May-01 June 2007, Jeju, South Korea, 293.

[T13] P.W. Egolf, A. Kitanovski, D. Vuarnoz, M. Diebold, C. Gonin, **Magnetic heat pump with ground heat source: Optimized prototype**. Annual report for the Swiss Federal Office of Energy, 2007, 1-11.

[T14] D. Vuarnoz, A. Kitanovski, M. Diebold, F. Gendre, P.W. Egolf, **A magnetic heat pump with porous magneto caloric material.** Physica Status Solidi C, 4, No.12 (2007), 4552-4555.

[T15] A. Kitanovski, P.W. Egolf, **Magnetic heating, refrigeration and power conversion**. International Refrigeration and Air Conditioning Conference at Purdue, July 14-17, 2008. Paper ID 2298.

[T16] A. Kitanovski, D. Vuarnoz, M. Diebold, C. Gonin, P.W. Egolf, 2008. **Research on rotary porous wheel magnetic heat pumps in Switzerland**. Ninth International Energy Agency Heat Pump Conference 20-22 May, 2008, Zürich.

[T17] P.W. Egolf, A. Kitanovski, C. Gonin, D. Vuarnoz. **Magnetic heating, refrigeration and power conversion with porous wheel machines: Technologies to save and recreate exergy.** Invited presentation and paper at the "Seminario CTR Comitato Tecnico Refrigerazione, AI-CARR, Vicennza, Italy, 2008, 61-71.

[T18] P. W. Egolf, A. Kitanovski, D. Vuarnoz, C. Gonin, T. Swinnen, P. Repetti, A. Orita, J.-L. Beney, **Magnetische Wärmepumpe mit Erd-Wärme-Quelle: Optimierter Prototyp**. Annual report for the Swiss Federal Office of Energy, 2008, 1-12.

[T19] A. Kitanovski, C. Gonin, D. Vuarnoz, O. Sari, P.W. Egolf, **A standardization of the coefficient of performance and cost determination for magnetic refrigerators, heat pumps and power conversion machines**. Third IIR Int. Conf. on Magnetic Refrigeration at Room Temperature, Des Moines, USA, 12-15 May 2009, 229-237.